THE ASTROPHYSICAL JOURNAL, 347: L89–L92, 1989 December 15

STRUCTURE OF THE MAGNETIC FIELD IN THE W3 CORE

T. H. TROLAND
University of Kentucky
R. M. CRUTCHER
University of Illinois
W. M. GOSS
National Radio Astronomy Observatory
AND
C. HEILES
University of California, Berkeley
Received 1989 July 25; accepted 1989 September 14

ABSTRACT

We have mapped the Zeeman effect in the H I absorption line toward the W3 core with $\approx 1'$ resolution. The line-of-sight component of the magnetic field exceeds 100 μG and reverses direction. This morphology could be the result either of the collapse of the molecular cloud during the star formation process or of the action of an expanding H II region on the placental molecular gas.

Subject headings: interstellar: magnetic fields — stars: formation

I. INTRODUCTION

The importance of magnetic fields in star-forming molecular clouds is now widely appreciated. Unfortunately, empirical knowledge of magnetic field strengths in such regions has grown quite slowly. The only successful measurements have come from the Zeeman effect in radio frequency spectral lines, most notably those of H I and OH. Heiles (1987) and Crutcher (1988) have reviewed such observations, most of which have been made with single antennas. However, comparison between theory and observation is facilitated by observational data having high spatial resolution, such as that obtained by aperture synthesis techniques. This *Letter* reports VLA[1] OH and H I results for the core of the W3 region of massive star formation.

Verschuur (1970) attempted to observe the Zeeman effect in H I emission toward W3, but spurious signals in the V spectrum from H I emission in polarized telescope sidelobes dominated his result. Kazès and Crutcher (1986) reported a probable detection of the Zeeman effect in 1665 and 1667 MHz OH absorption lines toward W3. This result was limited not by sensitivity but by the presence of polarized OH masers. They derived a field strength of $+73 \pm 7$ μG by excluding from the analysis velocities with obvious masers. The VLA observations reported here use the spatial filtering property of an interferometer to suppress spurious effects: masers in the case of OH and spatially extended emission in the case of H I.

II. OBSERVATIONS

VLA observations of the 1420 MHz line of H I and of the 1667 MHz line of OH were carried out in 1984 October in the D configuration with a maximum baseline of 1 km. The pointing position was $\alpha_{1950} = 02^h21^m50^s$, $\delta_{1950} = 61°50'$. Channel 16 of the 31 spectrometer channels was centered at $V_{LSR} = -40.875$ km s^{-1}, and channel separation was 3.05 kHz (0.64 km s^{-1} at 21 cm). The single circular polarization sense of the array was switched every 5 minutes.

Channel maps with 15″ pixels were made separately for right (R) and left (L) circular polarization. The synthesized beams have half-power widths of 66″ × 53″ at 21 cm and 57″ × 46″ at 18 cm with a position angle of 105°. In order not to introduce possible spurious effects in the V spectra, no deconvolution of the synthesized "dirty" beam from the maps was carried out. Because the very strong W3(OH) maser was near the half-power point of a single-dish beam, radiation from this maser affected the entire map in several spectral channels. This interference was suppressed by subtracting the beam point-spread function at the position of the maser from the OH maps. However, the expectation of eliminating polarized maser signals from the OH V spectra was not realized. Spectra at every pixel show clear evidence of circularly polarized emission. Apparently there are many weak maser spots throughout the W3 core area. Because of maser contamination, we cannot rely upon the OH VLA observations.

For the H I data, channel maps of $I = (R + L)/2$ and $V = R - 1.037L$ were constructed, and I and V spectra were extracted for each pixel in the central region of the maps. The gain correction factor (1.037) was determined empirically by the requirement that scaled-down replicas of the I spectra not appear in the V spectra.

Figure 1 shows H I and OH I spectra and the H I V spectrum for a single pixel near the continuum peak. Goss *et al.* (1983) produced higher resolution maps of H I absorption toward W3 and found that the H I absorption within the velocity range sampled consists of components at $V_{LSR} \approx -38.5$, -43.5, and -48.0 km s^{-1}. The OH absorption line in Figure 1 (which is a single absorption line with a polarized weak maser line at the center rather than the double absorption line it appears to be) occurs at about -38.5 km s^{-1}.

The only significant signal in the H I V spectrum (Fig. 1) is a negative feature near -33.5 km s^{-1}. The signature of a uniform line of sight magnetic field is a signal in the V spectrum with the shape of the derivative of the I spectrum. If the

[1] The VLA is a facility of the National Radio Astronomy Observatory which is operated by Associated Universities, Inc. under cooperative agreement with the National Science Foundation.

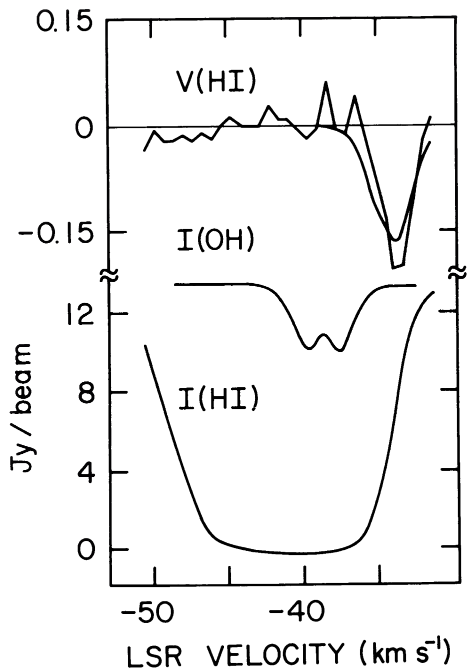

FIG. 1.—VLA line profiles towards $\alpha(1950) = 2^h21^m56^s$, $\delta(1950) = 61°53'$. The bottom two spectra are H I and OH line profiles. Above these is the observed H I V spectrum (jagged line), with the derivative of the I spectrum (scaled to the derived $B = 66.5$ μG) superposed.

entire H I absorption line arose in a region of uniform magnetic field, the negative feature in the V spectrum should have a corresponding positive feature near -49 km s^{-1}. If the three H I components correspond to different clouds and only the -38.5 km s^{-1} cloud has a significant line-of-sight field, then the negative feature observed in the V spectrum near -33.5 km s^{-1} should have a corresponding positive feature at about -43.5 km s^{-1}, that is, near the center of the adjacent H I component. However, high optical depth in the adjacent component should suppress this positive feature in the V spectrum and may even suppress by as much as 10% the observed negative feature near -33.5 km s^{-1}.

We have derived the line-of-sight magnetic field strength at each pixel in the H I maps for the high-velocity wing of the -38.5 km s^{-1} component. We have done so on a channel-by-channel basis, dividing the observed V spectrum at each channel by the numerical derivative of the I spectrum (see Schwarz *et al.* 1986). We calculated the rms uncertainty in the field strength for each channel by assuming that the scatter about zero of the observed V spectrum for channels with $V_{LSR} < -40$ km s^{-1} was due to random noise. The data have insufficient sensitivity to investigate variations of field strength with velocity. Therefore, we calculated the average field strength at each position from the individual channel values, weighted by the inverse square of the error for each channel value. Figure 2 shows V spectra at 30″ intervals for the W3 core. Above each spectrum is the derived magnetic field strength and the 1 σ error, the latter computed via standard statistical techniques. The I spectra for this region vary in strength, but variations in line shape or velocity are slight. Hence, the derived field in each pixel is nearly proportional to the amplitude of the Zeeman signal divided by the strength of the I spectrum, and the error in the field in each pixel varies inversely with the strength of the I spectrum. The feature at the right side of the V spectra, which we attribute to the Zeeman effect, changes from negative to positive from the northeast to the southwest. This fact implies a reversal in the field direction over the W3 core. A negative field value points toward the Sun.

III. DISCUSSION

The W3 region has been intensively studied. From the H I synthesis study of Goss *et al.* (1983), the molecular studies of Dickel *et al.* (1980) and Dickel (1980), and the radio continuum and recombination line studies of Roelfsema (1987), among others, W3 is known to be a giant complex of recent star formation in the Perseus arm ($l = 133°.7$, $b = +1°.2$) about 2 kpc from the Sun. The mass of the molecular complex is $\sim 10^5$ $M_\odot$, most of which is in the low-density extended molecular cloud. The main core of the W3 cloud (shown in Fig. 3) is

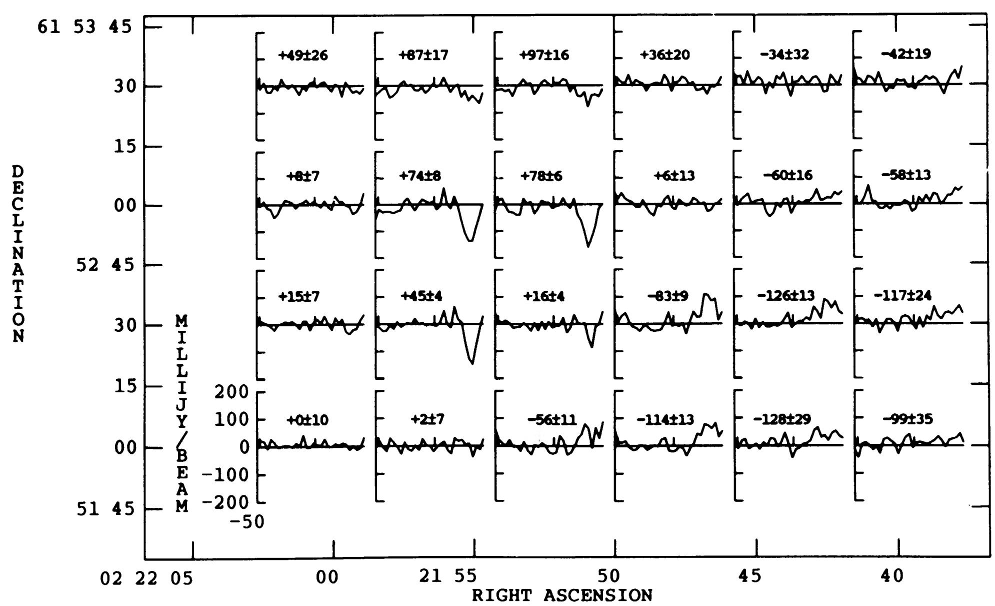

FIG. 2.—Observed V spectra with derived magnetic fields and 1 σ errors (in μG). The intersection of the coordinates axes marks the sky position for each spectrum.

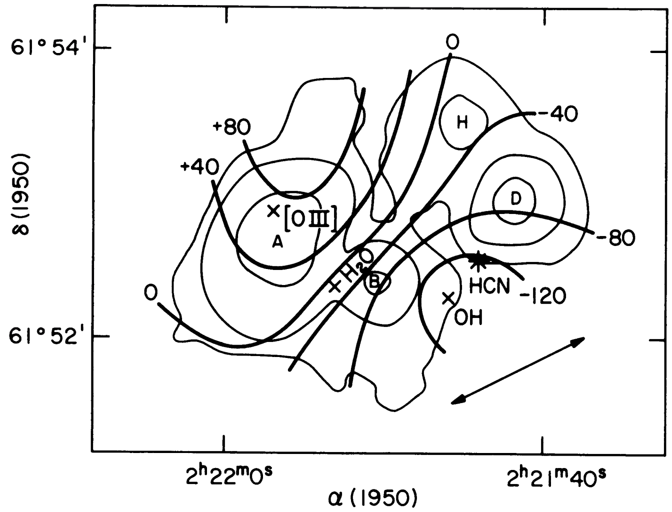

FIG. 3.—Contours (*heavy lines*) of the line-of-sight component of the magnetic field derived from the H I line, in μG. Selected contour (*light lines*) of the 21 cm continuum map from Dickel *et al.* (1980) are shown. X's mark the locations of H_2O and 1720 MHz OH masers and the peak of the optical [O III] jet, and a star marks the center of the Hat Creek HCN cloud. The line to the lower right indicates the direction of the magnetic field in the plane of the sky from optical polarization studies.

centered near $\alpha_{1950} = 02^h21^m44^s$, $\delta_{1950} = 61°52'32''$, with diameter of $\sim 5'$ or ~ 3 pc. The mean H_2 density in the core is $\sim 2 \times 10^4$ cm^{-3}, and the molecular mass is $\sim 10^4$ $M_\odot$. The mean molecular velocity of the core is about -40 km s^{-1}, with a gradient of about $+2$ km s^{-1} arcmin^{-1} from southeast to northwest. The center of the molecular core is well defined by a high-density HCN cloud with diameter $\sim 40''$ (0.4 pc) mapped with the Hat Creek interferometer (Wright, Dickel, and Ho 1984).

Within the W3 molecular core is a group of compact H I regions (A through H) at various stages of evolution. The most evolved is A, which has the morphology of a partial shell. The mean velocity is $V_{LSR} \approx -40$ km s^{-1}, and the shell appears to be expanding at ~ 2–3 km s^{-1}. In addition, a broad H166α line with $V_{LSR} \approx -59$ km s^{-1} is observed, which suggests that the H II region has broken through the surrounding neutral gas and that low-density ionized gas is flowing toward the Sun. That this flow is from the northern part of region A is suggested by the presence of an Hα and [O III] optical "jet" just north of the shell center and also by H_2CO absorption which is strong over the southern part of region A and very weak toward the north. The compact H II regions lie mostly to the east and northeast of the center of the W3 molecular core.

Also associated with the W3 complex is the H I observed in 21 cm absorption. Goss *et al.* (1983) argue that the -38.5 and -43.5 km s^{-1} components arise in shells surrounding the compact H II regions where H_2 has been photodissociated. The H I component at -38.5 km s^{-1} corresponds closely in velocity with the OH absorption (Fig. 1); therefore, the H I may be closely associated with molecular gas. In the context of the shock models of Hill and Hollenbach (1978), this H I component may arise in (dissociated) preshock gas, while the -43.5 km s^{-1} H I component arises in postshock gas. In this case, the H I Zeeman effect in the -38.5 km s^{-1} component is representative of magnetic fields in the molecular cloud before the onset of star formation. Alternatively, the -38.5 km s^{-1} component may arise in postshock gas, in which case the field strength has likely been enhanced by shock compression.

Figure 3 shows a representation (from Dickel *et al.* 1980, with higher angular resolution than our data) of the 21 cm continuum image of the W3 core; the positions of the stronger compact H II regions (A, B, D, and H), the [O III] jet, H_2O and OH masers, and the core center as defined by HCN are indicated. We have superposed contours of the line-of-sight component of the magnetic field derived from our H I observations. Also shown is the direction of the magnetic field in the plane of the sky derived from optical polarization measurements (Lanzen, Schulz, and Schmidt 1981).

The line-of-sight component of the magnetic field toward the W3 core has a striking property: *it reverses direction.* One simple explanation comes from considering the morphology of a frozen-in field in a collapsing cloud. In the simplest case, the gas will collapse preferentially along the field to form a disk, although some collapse will also occur perpendicular to the field. Field lines will be drawn into an hourglass shape, with the disk eventually fragmenting and forming stars and compact H II regions. If the original field lay in the plane of the sky, the distorted field *in front* of the H II region (where absorption lines arise) would reverse direction, and the long axis of the disk would be the locus of zero line-of-sight field (zero locus). The magnetic field would have its maximum total strength near the zero locus, where the field is entirely in the plane of the sky. Therefore, this maximum could be much higher than the ~ 100 μG line of sight component we measure.

There are two problems with this model: (1) The zero locus should pass through the center of the W3 core. If the present center of the molecular core were the original center before star formation began, this expectation is not met. However, the simple picture falls far short of representing the complexity of the W3 region. Also, if the original field were not perfectly in the plane of the sky, then the zero locus would be displaced from the molecular disk. (2) The direction of the field in the plane of the sky should be perpendicular to the zero locus. The optical polarization data give an angle of only 20°. This apparent contradiction may not be serious since the polarization angle is based on only a few stars, none of which samples the dense gas of the W3 molecular core. Observations of the linear polarization of IR radiation from hot grains in the core would allow a more relevant comparison with this simple model.

Another explanation for the field reversal is that star formation activity has modified the morphology of the magnetic field. The two local maxima of the field are near the molecular core center position and near the [O III] jet, where the compact H II region may be in a champagne flow toward the Sun. Perhaps before star formation, the field was uniform in direction but neither parallel nor perpendicular to the light of sight. The expansion and subsequent champagne flow of H II region A pushed the frozen-in field toward the Sun and reversed the direction of the line-of-sight component. A problem with this scenario is that the H I velocity in the northern part of region A should be more negative by ~ 2–3 km s^{-1} (the expansion rate of the ionized shell) than toward other positions. No such velocity difference is, in fact, observed.

IV. CONCLUSIONS

Whatever the detailed explanation for field reversal in the complex WC core region, the discovery of such a reversal underscores the importance of high angular resolution studies in understanding the role of magnetic fields in star-forming regions. Indeed, synthesis studies are clearly of value even for star-forming regions which yield only upper limits in single-dish Zeeman effect observations. The example of W3 is particularly relevant not only because field reversal exists in the H I gas, but also because the H I velocity component in which the field has been detected may arise in dissociated but otherwise undisturbed gas in the molecular cloud. Therefore, although the Zeeman measurement is in H I, the result may be directly relevant to field strengths in the molecular cloud itself.

The relevance of the present measurement to molecular clouds is underscored by the rather high field strengths detected, of order 100 μG. Such fields are typical of those encountered in single-dish OH Zeeman effect studies of molecular clouds with embedded high-mass stars (Crutcher 1988). Therefore, the present result augments the growing evidence that field strengths in such regions are systematically higher than in dark clouds and similar cold molecular clouds that do not produce massive stars.

T. H. T., R. M. C., and C. E. H. acknowledge partial support of this research by NSF grants AST-8611887 and AST-8817651.

REFERENCES

Crutcher, R. M. 1988, in *Molecular Clouds in the Milky Way and External Galaxies*, ed. R. L. Dickman, R. L. Snell, and J. S. Young (Berlin: Springer-Verlag), p. 105.
Dickel, H. R. 1980, *Ap. J.*, **238**, 829.
Dickel, H. R., Dickel, J. R., Wilson, W. J., and Werner, M. W. 1980, *Ap. J.*, **237**, 711.
Goss, W. M., Retallack, D. S., Felli, M., and Shaver, P. A. 1983, *Astr. Ap.*, **117**, 115.
Heiles, C. E. 1987, in *Interstellar Processes*, ed. D. Hollenbach and H. Thronson (Dordrecht: Reidel), p. 171.
Hill, J. K. and Hollenbach, D. J. 1978, *Ap. J.*, **225**, 390.
Kazès, I., and Crutcher, R. M. 1986, *Astr. Ap.*, **164**, 328.
Lenzen, R., Schulz, A., and Schmidt, Th. 1981, *Astr. Ap.*, **100**, 249.
Roelfsema, P. R. 1987, Ph.D. thesis, University of Groningen.
Schwarz, U. J., Troland, T. H., Albinson, J. S., Bregman, J. D., Goss, W. M., and Heiles, C. 1986, *Ap. J.*, **301**, 320.
Verschuur, G. L. 1970, *Ap. J.*, **161**, 867.
Wright, M. C. H., Dickel, H. R., and Ho, P. T. P. 1984, *Ap. J. (Letters)*, **281**, L71.

R. M. Crutcher: Astronomy Department, University of Illinois, Urbana, IL 61801

W. M. Goss: NRAO, P.O. Box O, Socorro, NM 87801

C. Heiles: Astronomy Department, University of California, Berkeley, CA 94720

T. H. Troland: Physics and Astronomy Department, University of Kentucky, Lexington, KY 40506